Tellus (1991), *43A*, 306–320

Quantitative comparison between simulated cloudiness and clouds objectively derived from satellite data*

By ELMER RAUSTEIN, *Geophysical Institute, University of Bergen Allégt. 70, N-5007 Bergen, Norway*, HILDING SUNDQVIST, *Department of Meteorology, Stockholm University S-106 91 Stockholm, Sweden* and KRISTINA B. KATSAROS, *Department of Atm Sciences, University of Washington Seattle, WA 98195, USA*

(Manuscript received 7 August 1990; in final form 8 January 1991)

ABSTRACT

The cloud cover and cloud water content obtained from integration of a limited area mesoscale prediction model are compared with the corresponding quantities derived from AVHRR and SSM/I satellite data. The model has an elaborate condensation-cloud parameterization scheme, in which cloud water is a prognostic variable. From AVHRR data, both cloud cover and liquid water content are retrieved by utilization of radiances from the visible, near infrared and infrared channels. From the 37GHz polarization difference in the microwave data obtained from SSM/I measurements, liquid water content is interpreted; this is only possible over the sea. An important feature of this comparison exercise is that the retrieved data are distributed on the same grid as the model. The difference between the simulation and the analysed cloud fields can thus easily be quantified and exhibited on the model domain. It is demonstrated that this type of retrieved meteorological parameters constitutes potentially useful data samples for quantitative verification of model simulations. There are some weaknesses in the retrieval methods that have to be removed before we can have sufficient confidence in the data to make quantitative verification meaningful. Furthermore, calibration against cloud parameters obtained through other measurements is necessary, although the three data sets show a remarkably good agreement in pattern and range of magnitude in the liquid water content. Even if improvements are needed, the present study has made it possible to make inferences about some deficiencies in the parameterization scheme of the model.

1. Introduction

During the past decade, a great number of numerical model studies have been devoted to investigation of sensitivity to cloud-radiation conditions in the atmosphere. By and large, it can be said that all those studies indicate that there is an important impact from the cloudiness on the resulting circulation in NWP models and GCM (see list of acronyms in Appendix) as well as in climate models (Manabe and Stouffer, 1980; Ramanathan et al., 1983; Röckner and Schlese, 1987; Wetherald and Manabe, 1988; Cess et al., 1989; Slingo, 1990). It can furthermore be stated that very little attention generally is paid to the model clouds themselves. With regard to the sensitivity to clouds, it is urgent that much more work be done on the problem of condensation-cloud parameterization. The more realistic the model cloudiness becomes, the more confidently we can draw conclusions from model results. In the most recent papers, a concern may be found about the realism in the model cloud fields (Wetherald and Manabe, 1988; Cess et al., 1989).

There are two aspects that must be considered in a parameterization problem. One is the derivation and development of parameterization schemes, the other is the verification that model results exhibit

* Contribution number 625.

a realistic behavior and distribution of, in this case, cloudiness.

The conventional ground-based cloud observations are incomplete and spatially too sparse to constitute a useful data set in the context discussed here. It is not until recently that relevant observational data have become available through satellite measurements. From the AVHRR data, it is now possible to make quantified interpretations of cloud cover and cloud water content (Raustein, 1989). From the microwave measurements, quantified cloud water content and precipitating water content may be deduced (Staelin et al., 1976; McMurdie and Katsaros, 1985; Takeda and Liu, 1987; Katsaros et al., 1989; Petty, 1990; Curry et al., 1990; Katsaros et al., 1990).

The satellite measurements also have their limitations. Cloud classification from AVHRR data utilizes channels both in the infrared (IR), and in the visible part of the spectrum. The interpretations are sensitive to sun elevation, and criteria for distinguishing between clouds and snow are not currently included in the method. Furthermore, microwave data can only be used over ocean areas.

The interpretation of both AVHRR data and microwave data are in an early stage of development. This means that the "observations" obtained this way have some degree of uncertainty, especially in absolute values.

There is another important aspect that is common to all of these satellite measurements. Namely, they give the vertically integrated value of the measured quantities. These do not necessarily reflect a unique vertical distribution (Slingo and Slingo, 1988).

Because of the development stage of the interpretation schemes and because of the two-dimensionality of the measurements, it is important that we utilize as many categories of measurements as possible for the model verifications. A careful comparison of corresponding measurements by different methods, as well as comparison of model results and measurements, may assist in calibrating the observations. In this way an enhanced confidence in the observations may gradually be achieved.

In order to verify simulated vertical distributions, it hence appears necessary to obtain observations also in other ways, such as from dedicated field programs such as, for example, FIRE (Cox et al., 1987). Then, as condensation-cloud parameterization schemes begin to show an acceptable performance, those schemes can be utilized to infer vertical distributions from satellite measurements.

There is a long way to go before we have reached a satisfactory state with regard to observational data of condensation-cloud quantities, as well as a realistic simulation of those quantities in various models. Considering the attention the cloud topic has gained recently, it is indeed urgent to intensify the research efforts in both modelling of condensation-cloud processes and in the verification of those simulations.

We are therefore of the opinion that, at the present state of the art, cloud parameters, derived from satellite data, are not yet quite ready to be used for direct absolute verification of model simulations. But to improve this situation, it is necessary to go through a development phase, in which we make comparisons between interpreted variables and model variables. This is the purpose of the present paper. A study along similar lines has recently been published by Saunders (1989).

The simulated cloudiness is produced in a NWP model (the AMUB model, which is a version of the operational model of the Norwegian Weather Service, modified at the University of Bergen), which has an elaborate condensation-cloud parameterization scheme.

The observed cloud parameters are obtained from two sources. One comprises cloud cover and vertically integrated liquid water content, objectively derived from satellite AVHRR data according to the approach suggested by Raustein (1989). The other data set is vertically integrated liquid water content, which is obtained by interpretation of satellite microwave measurements according to Petty (1990).

One model field which would have been desirable to compare to a corresponding satellite data field, is that of total outgoing longwave radiation. However, this field is not available from the satellite data we are using, as they are taken only from a few window bands.

Specifically, comparisons are made between clouds, predicted with the AMUB model and satellite clouds at times differing by not more than half an hour to one hour. An important feature of this study is that the cloud parameters from the

satellite data are projected on the same grid as the model.

2. Model features and the derivation of cloudiness from AVHRR and SSM/I microwave data

2.1. Model features

The AMUB model is a modified version of the operational fine mesh model at the Norwegian Weather service (DNMI). A description of the original version may be found in Grønås et al. (1987) and Nordeng (1986). The modifications introduced at AMUB are described by Sundqvist et al. (1989). Consequently, here we only present the broad features of the AMUB model. This limited area model is based on the primitive equations with sigma as vertical coordinate. In the experiments presented here, the horizontal resolution is 50 km and there are 10 levels in the vertical, with the top at 200 mb. The number of grid points at each level is 49×61; the geographical area that is covered may be seen in Fig. 4.

The time integration is explicit, but the scheme contains spatial and temporal smoothing of the tendencies in the staggered grid so that the time step is nearly four times as long as the one basically obtained from the CFL condition (Bratseth, 1983). Vertical eddy diffusion is applied through the whole depth of the model atmosphere. The exchange coefficient is a function of the Richardson number and cloud cover. The sea surface temperature is prescribed, while over land, an energy exchange equation is applied as well as a soil moisture formulation, accounting for precipitation, storage and run off. Radiative fluxes are calculated at all model levels. The fluxes are modified with regard to the current cloud cover obtained from the condensation-cloud parameterization. The emissivities are not functions of the cloud water content, but prescribed with different values for high, medium high and low clouds.

As indicated, the particular feature of the AMUB model is that an elaborate condensation-cloud parameterization scheme is employed. This scheme carries cloud water as a prognostic variable and treats release of latent heat, appearance of fractional cloud cover, cloud water content and precipitation/evaporation in a consistent way (Sundqvist, 1988; Sundqvist et al., 1989).

The parameterization of the *microphysical processes* accounts for coalescence as well as Bergeron-Findeisen effects. This scheme is *common for convective and stratiform* condensation, but the associated parameters have different values in the two stability regimes.

For the parameterization of *convective condensation*, a modified Kuo scheme is employed. The scheme includes calculation of cloud water. The partitioning of converging vapour between moistening and condensation is essentially governed by the relative humidity. The fractional cloud cover is a function of the intensity and the depth of the convection. The condition for *stratiform condensation* to appear is that the relative humidity is greater than a prescribed threshold value, which is different over sea and land. The fractional cloud cover is a linear function of the square root of the sub-saturation. The *cloud water advection*, which is only horizontal, is calculated with an upstream scheme to assure positive definite cloud water values.

2.2. Derivation of cloud parameters from AVHRR data

The method of deriving fractional cloud cover and vertically integrated liquid water content (LWC) is described by Raustein (1989). A brief description of the method is given below.

Three of the AVHRR channels are utilized, viz. *channel 1* (0.58–0.68 μm, visible), *channel 2* (0.7–1.1 μm, near infrared), and *channel 4* (10.5–11.5 μm, infrared). First a statistical method called clustering is applied to the data of channels 1 and 4 to obtain an objective cloud classification. In the two-dimensional radiance space, we find concentrations of pixels (called clusters), which we identify as certain cloud types, or as either land or sea surface. Pixels belonging to a certain cluster contain clouds of the same type, and the area covered by such a pixel is assumed to be overcast. Pixels that are scattered and thus not belonging to a cluster are overcast or partially cloudy. The cloud fraction of such a pixel is found in two steps: (a) The cloud type, to which the clouds in the pixel belong, is obtained by finding the cloud cluster, to which the pixel is closest in the 3-dimensional radiance space, where the 3 dimensions are the radiances of channels 1, 2 and 4. (b) The cloud

fraction is then found by linearly interpolating the pixel's channel 2 radiance between the surface cluster's mean, and the closest cloud cluster's.

To compute the LWC and cloud top temperature we use radiative transfer models of Coakley and Chylek (1975) and Arking and Childs (1985), together with parameterized LWC and channel 4 emissivity according to Stephens (1978).

In order to have the cloud parameters derived from the satellite data projected on the same grid as the model, a navigation method developed by Kloster at NRSC (personal communication) is used to position each pixel in the model grid. The grid box value of each cloud parameter is then taken as the average of the values of the pixels which belong to the grid box.

2.3. *Derivation of liquid water content from microwave data*

The microwave data are from the SSM/I on the F8 satellite in the US Defense Meteorological Satellite Program (DMSP), which was launched into a polar orbit in June 1987. This microwave radiometer scans a 1390 km wide swath in a conical sweep at 53° incidence angle. Operating frequencies are 19.35, 22.235, 37 and 85.5 GHz, in both horizontal and vertical polarization, except the 22.235 GHz channel, which only operates in horizontal polarization. The pixel resolution is nominally 50, 50, 25 and 15 km, respectively. Several possible algorithms for determining cloud liquid water content have been developed (e.g., Petty, 1990). For the purpose of this model-satellite data comparison, a 50-km resolution-integrated cloud liquid water algorithm based on the 37 GHz polarization was selected. For higher spatial resolution and better discrimination, an algorithm employing the 85.5 GHz channels has been developed (Petty, 1990). Unfortunately, this algorithm cannot be used for our August 1988 case, due to gain problems with the 85.5 GHz channel in vertical polarization, which had started shortly before this time.

The 37 GHz algorithm is based on the theoretical depolarization effect of the cloud droplets on the polarized emission from the sea surface. A relation between the observed polarized signal, P, and vertically integrated liquid water mass, L ($\equiv$ LWC), is of the following form (Petty, 1990):

$$P = \tau_l^{\alpha} = \exp\left[-\frac{\alpha\kappa L}{\cos\theta}\right], \tag{2.1}$$

where τ_l is effective, microwave transmittance associated with the cloud liquid water, α has the approximate value 2, κ is effective mass extinction coefficient of the liquid water in the cloud and θ is the incidence angle (53°).

The relation for L_{37} in terms of polarization at 37 GHz ($T_{37V} - T_{37H}$) has been found from a theoretical brightness temperature model, which provides values for $\alpha \cdot \kappa$:

$$L_{37} = -1.42 \ln(P_{37}) \qquad (\mathrm{kg\,m^{-2}}). \tag{2.2}$$

P_{37} includes corrections for changes in the background, that is the wind roughening of the sea surface and water vapour in the column. Thus

$$P_{37} = (T_{37V} - T_{37H}) \times \exp(0.151U + 0.00607V - 4.40), \tag{2.3}$$

where U is surface wind speed and V is water vapour content (SI units), also available from SSM/I brightness temperatures. Further details on the derivation of the complete and self-consistent set of algorithms developed to interpret SSM/I data are found in Petty (1990). Similar approaches to derive liquid water amount from microwave data are reported in Curry et al. (1990) and Takeda and Liu (1987).

It is pertinent to note that the liquid water content (LWC) derived from AVHRR as well as from microwave data comprise both cloud water and precipitating water. Thus there are reasons to expect that the analysed amounts should tend to be somewhat larger than the vertical integral of the simulated water content, which stems only from the clouds. We use the notation LWC both for analysed and simulated amounts, even if the latter ones strictly could be called cloud water content (CWC).

3. Comparison of model clouds and clouds derived from satellite measurements

3.1. *Choice of situation*

As mentioned above, there may be difficulties in the interpretation of AVHRR data at low sun

elevations and over snow covered surfaces. We have taken those aspects into account in our choice of situation for this first comparison. Furthermore, in order to make use of microwave data, we have looked for a cloud system that has its major parts over the sea surface during the period of comparison. This implies that there are very few conventional surface observations available for verification. We also wanted to find a situation with a pronounced non-stationary cloud system under motion during the simulation period.

Thus, we are considering a situation with initial time at 26 August 1988 12 GMT and the 30 h forecast (till 27 August 1988 18 GMT). The synoptic surface map is shown in Fig. 1. During this period, we have AVHRR data centred around 27 August 1988 8.45 GMT (Fig. 2), which we call Sav1 in the sequel, corresponding to +21 h simulation time, and 27 August 1988, 14.30 GMT (Fig. 3), Sav2, corresponding to +27 h. We have microwave data centred around three different points in time, one at 26 August 1988, 19.00 GMT, (around +6 h), another at 27 August 1988, 4.30 GMT, (around +16 h) and a third one from 18.30 GMT, (around +30 h); the last mentioned we call Smi3. It may be pointed out that in all those cases, the extracted satellite data cover only part of the computational area.

3.2. *Cloud cover from model and AVHRR measurements*

The cloud cover in the forecast model is defined at each level, so we have to calculate a 2-dimensional field of the cover, corresponding to what a satellite sees. There are three basic alternatives for such a calculation, namely, assumptions that clouds at different levels have either minimum, maximum or random overlap. There is of course some arbitrariness in each of the options. According to a recent study by Tian and Curry (1989), the two last mentioned alternatives are more realistic than the first one. We have adopted a maximum/random overlap assumption, imply-

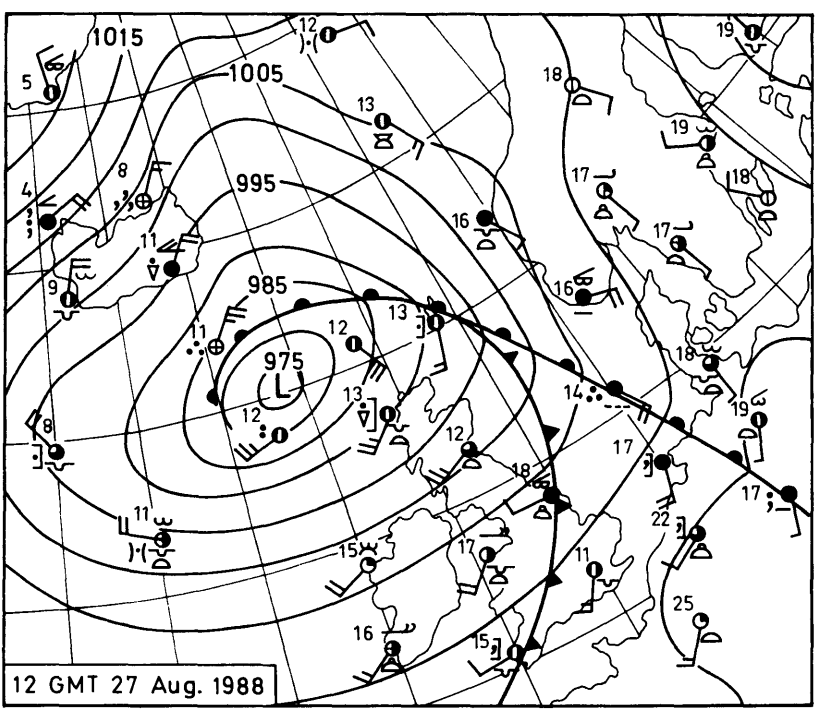

Fig. 1. Surface analysis at 12 GMT 27 August 1988.

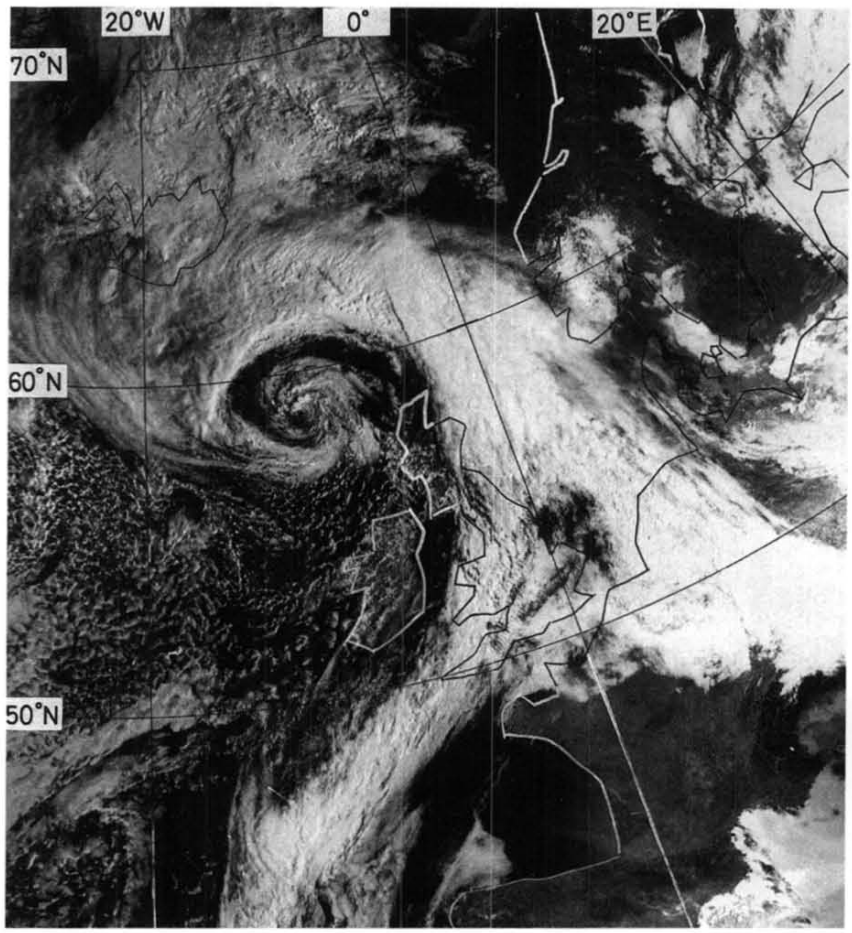

Fig. 2. Satellite (NOAA 10) picture in near infrared (channel 2) from passage 27 August 1988 around 8.45 GMT. (Satellite Receiving Station, Dundee University, UK.)

ing that maximum overlap is used as long as the cover varies monotonically from level to level in a column and that random overlap is taken when non-monotonic variation occurs in the same column (Sundqvist et al., 1989).

Figures 4a–b show that there is good overall agreement between Sav1 and the simulated cover at the corresponding time. One of the first things that we notice is that the satellite analysis has a somewhat larger overcast area than the model field. This disagreement is seen over the Gulf of Bothnia and over the area behind the cold front east of Scotland-England where the clear area is more extended in the model field than in the analysis. A corresponding deviation is also found south-west of Ireland. The synoptic map shows that a frontal wave is under development in this area. To see those differences quantitatively, we have subtracted the model cloud cover from the observed one in Fig. 4c. The differences mentioned above are clearly seen in this figure. These deviations, where the analysis shows practically overcast while the model field is cloud-free, could possibly be due to an uncertainty in the condensation scheme as to what the (threshold) conditions should be for condensation to appear. But it seems more likely that those deviations are due to the model dynamics, which may fail in simulating

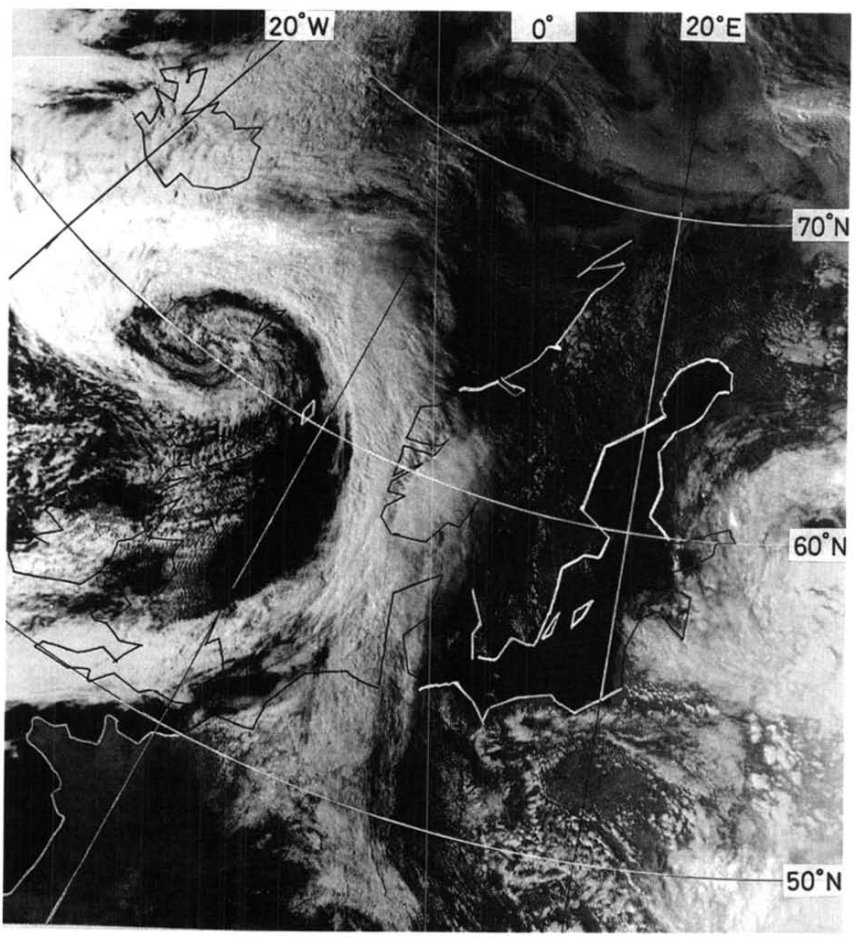

Fig. 3. Satellite (NOAA 9) picture in near infrared (channel 2) from passage 27 August 1988 around 14.30 GMT. (Satellite Receiving Station, Dundee University, UK.)

realistically the motions connected with (a) the fairly weak pressure gradients through a great depth over central Sweden and the Gulf of Bothnia, (b) the relatively small scale features behind the cold front, and (c) the developing wave entering through the southern boundary of the model area.

In the south-west sector of the low, where convection is taking place (Fig. 2), there are somewhat more negative than positive differences (Fig. 4c). This is even more evident in the water amount difference as we will see below. The synoptic observations in Scotland and Ireland report shower activity with cloud cover between three and seven octas. These features indicate that the interpretation of the AVHRR data has more uncertainty over areas with scattered convection.

Near the northern boundary of the analysis region, the difference pattern, with its positive values to the north and negative values to the south, indicates that the model may have a phase error in this condensation system.

The narrow band of negative values, implying more clouds in the model than in the analysis, just north and west of the low pressure centre is also worth noting in Fig. 4c. Fig. 2 exhibits a narrow cloud-free band, which evidently cannot be resolved by the model. From Fig. 4b it is seen that

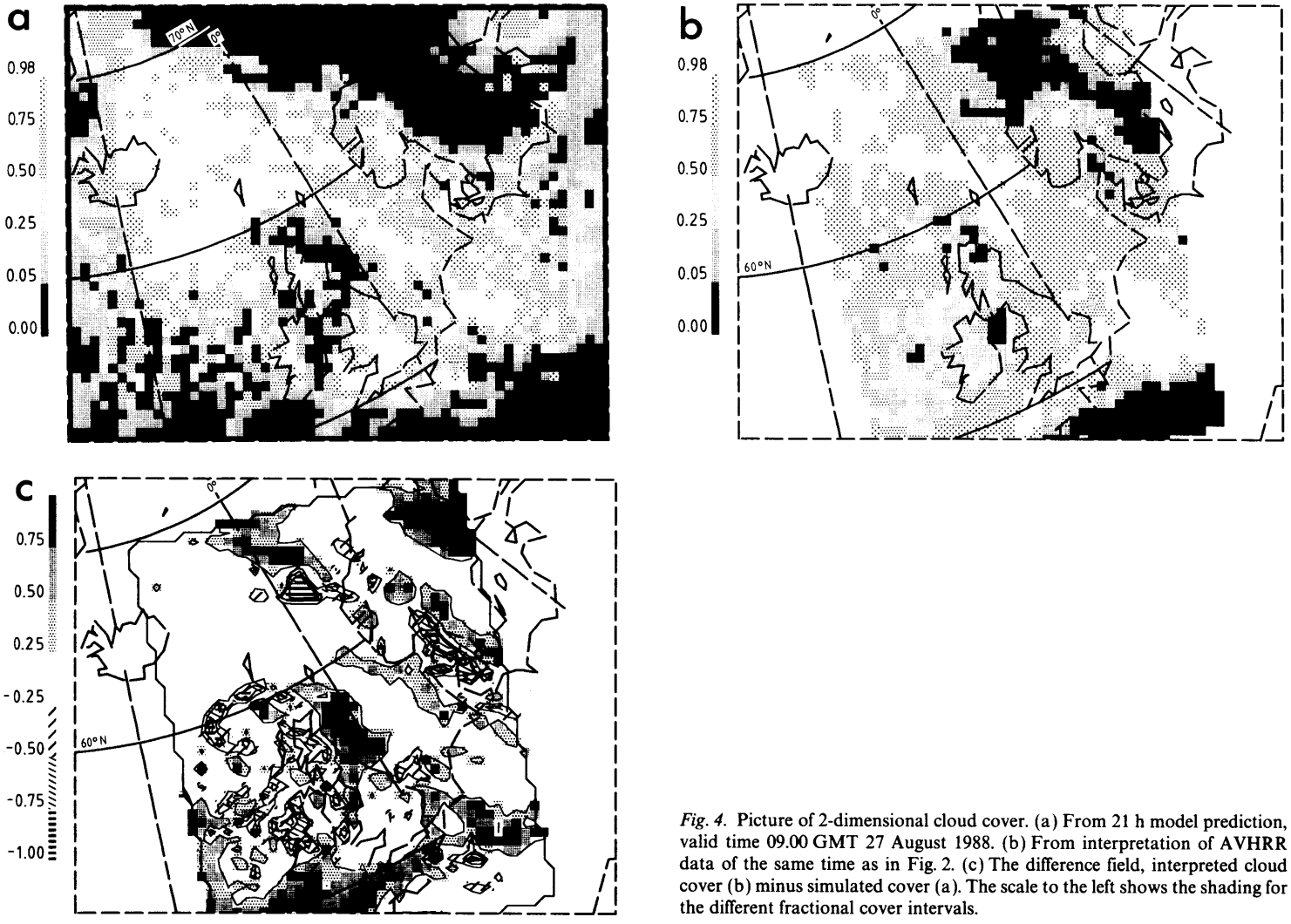

Fig. 4. Picture of 2-dimensional cloud cover. (a) From 21 h model prediction, valid time 09.00 GMT 27 August 1988. (b) From interpretation of AVHRR data of the same time as in Fig. 2. (c) The difference field, interpreted cloud cover (b) minus simulated cover (a). The scale to the left shows the shading for the different fractional cover intervals.

the analysis on the model resolution also loses the cloud-free feature and shows a partly cloudy band.

There are several areas with positive values in Fig. 4c that are interesting. As examples we may particularly regard the area along England's east coast, and the band beginning at 60° N and west of Norway and running toward SSE just west of Jutland into Western Germany. In these cases, the model simulates fractional cloudiness ranging between 25 and 75%, while the analysis shows a cover that systematically is 15–50 units larger. These discrepancies are probably due to the model's parameterization scheme for condensation. Thus, it is likely that the scheme tends to underestimate the *fractional stratiform* cloud cover.

We may also make a more statistical comparison by considering the following numbers: in the analysis area, the analysed clouds are present at 1560 gridpoints with an average cover of 66%, while the model clouds are present at 1310 gridpoints yielding a mean cover of 53%. Fig. 5 shows a frequency distribution of cloud cover categories for both the analysed clouds and the model clouds.

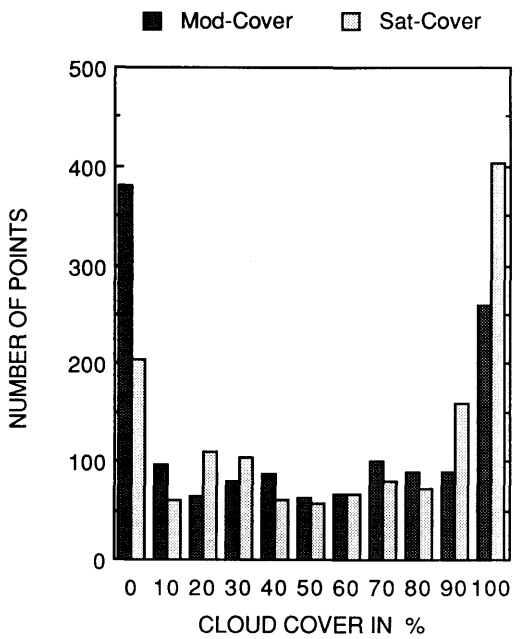

Fig. 5. Frequency distribution of cloud cover categories for the analysed clouds and the model clouds. The case is that of Sav2 and the forecast is for +27 h.

We have here chosen the time of Sav2, at which the comparison exhibits essentially the same results as those shown in Figs. 4a–c. From Fig. 5 we see that the analysed and the simulated cloud covers have an over all similarity in their bimodal distributions. But there are discrepancies, which are most pronounced in the extreme categories, that is, for zero and for 100%. There are markedly more cloudfree points and fewer overcast points in the simulated case than in the satellite analysis. This circumstance again shows the model's tendency to underestimate the cloud cover.

3.3. Cloud water content from model and AVHRR measurements

The satellite derived liquid water content is compared with the vertical integral of the predicted cloud water content. We noted earlier that the 2-dimensional cloud cover suffers from some arbitrariness due to the necessary assumption about overlapping; this is not the case with the vertically integrated water content, which is a well defined quantity.

As in the case of cloud cover, there is good qualitative agreement between the simulated cloud water field and the one obtained from the satellite measurements. Figs. 6a–b show that the simulated water content has a somewhat wider spread than found in Sav1, where the higher values appear in narrower bands. The maximum values are much the same, although there seems to be a few more points with the high values (more than 1.5 kg m^{-2}) in the Sav1 field (over Western Germany).

Fig. 6c shows the difference between the satellite derived water content and the model's vertically integrated cloud water amount. We may first observe the difference in the convection mentioned above in connection with convective cloud cover. In Fig. 6c, the simulated water amount is higher than the analysed amount over Scotland and western Ireland, and over the sea west of there. Regarding this discrepancy together with the synoptic reports and cloud cover differences shown above, it appears likely that the interpretation of the AVHRR data underestimates the convective cloud cover and water amount. There is also a band along the front from Cornwall toward ENE through England where the simulated water amount is higher than the analysed one, but in this

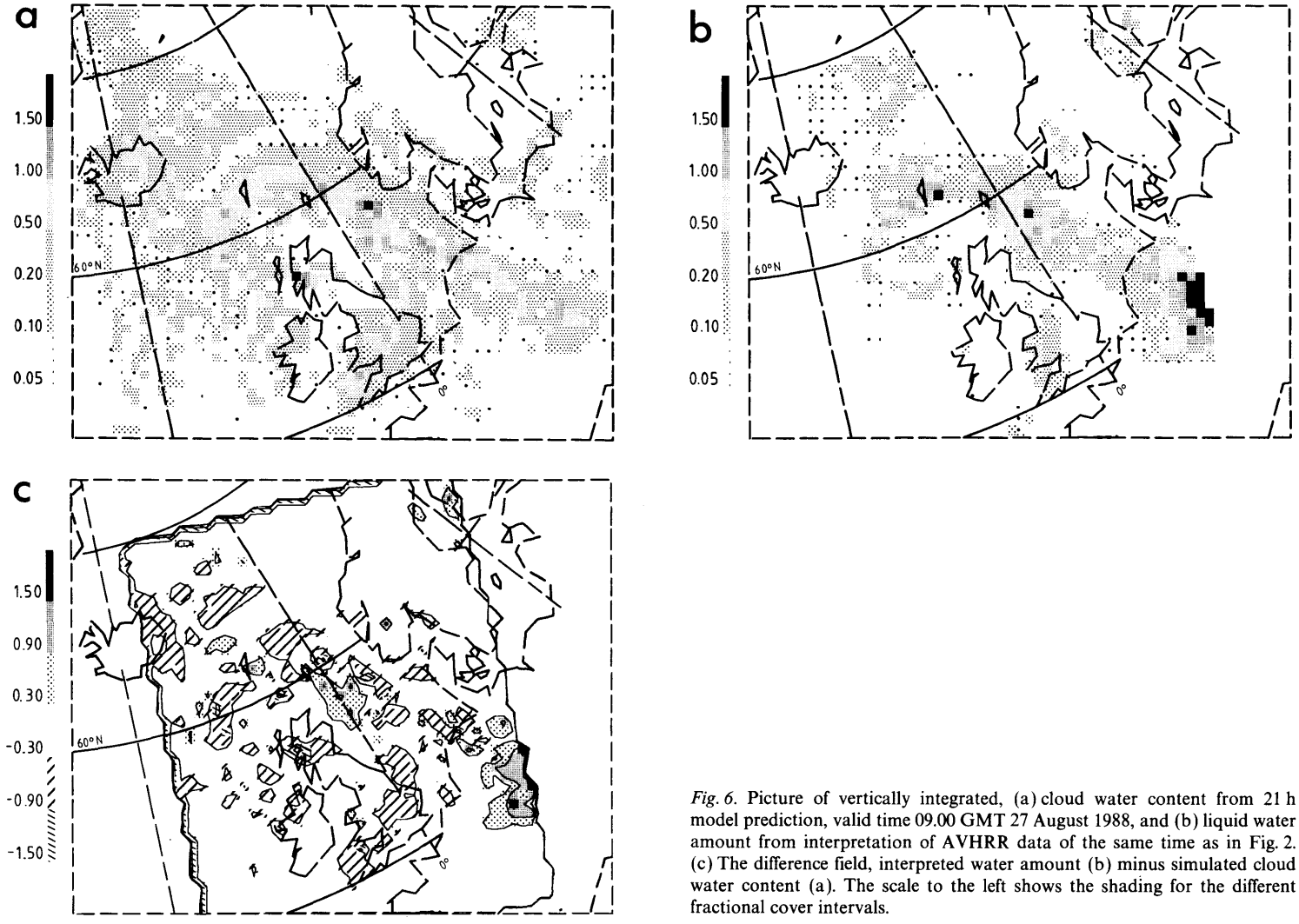

Fig. 6. Picture of vertically integrated, (a) cloud water content from 21 h model prediction, valid time 09.00 GMT 27 August 1988, and (b) liquid water amount from interpretation of AVHRR data of the same time as in Fig. 2. (c) The difference field, interpreted water amount (b) minus simulated cloud water content (a). The scale to the left shows the shading for the different fractional cover intervals.

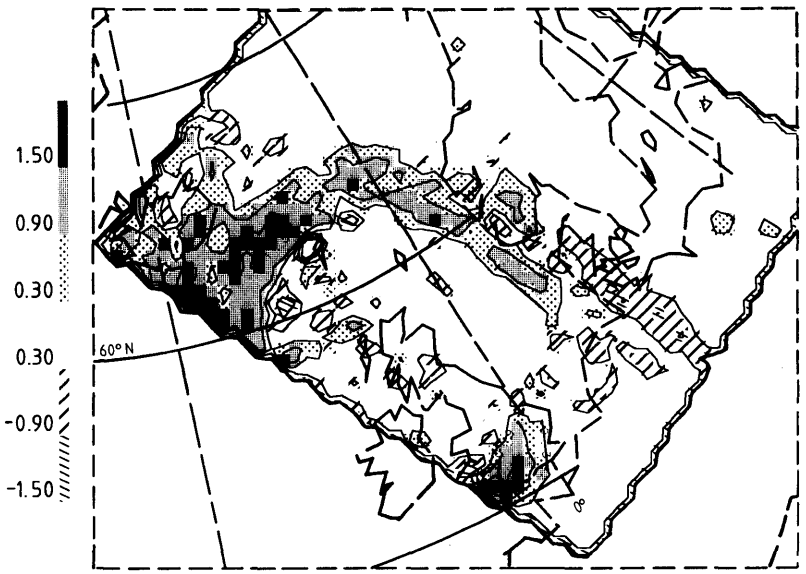

Fig. 7. The difference field, interpreted water amount at the time of Fig. 3, minus simulated cloud water content from +27 h of the model prediction. The scale to the left shows the shading for the different amount intervals; unit, $kg \cdot m^{-2}$, (or mm water column).

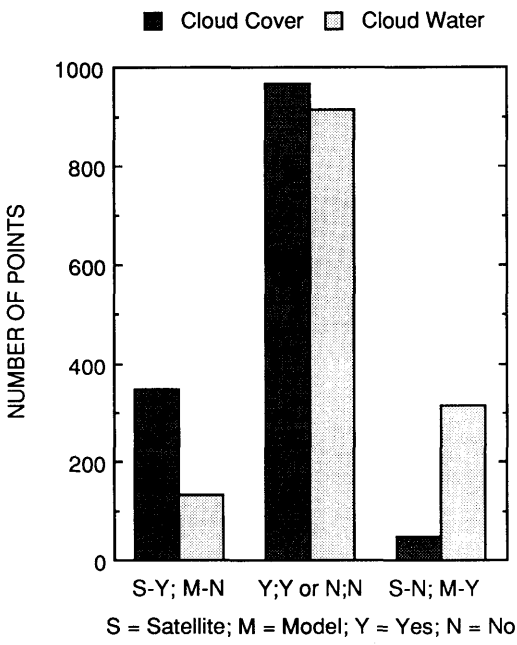

Fig. 8. The figure exhibits the number of grid points of agreement and of disagreement between observation and simulation for cloud cover and for cloud water content.

case it is more difficult to judge which of the two fields is the more realistic one.

At the time of Sav2, Fig. 7, there is a more distinct difference in the cloud water content, with the higher values in the measured field. However, there is better agreement in the spatial distribution than at the time of Sav1. The degree of spatial agreement at the time of Sav2 is indicated in another way in Fig. 8, which depicts the number of grid points of agreement and of disagreement between observation and simulation for cloud cover as well as for cloud water content. The figure also shows that the model underestimates cloud cover. Furthermore, the figure indicates that there is a discrepancy between the number of points with cloud cover and the number of points with cloud water. A slight contribution to this discrepancy may come from the model output, because the fields of cover and water differ by one time step. But the major contribution appears to come from the analyses, in which we found a distinct difference between Sav1 and Sav2 in spatial spread of cloud water. This question is directly connected to the matter discussed in the next paragraph.

There is one feature that is apparent when looking at Figs. 2 and 3, namely that the clouds appear

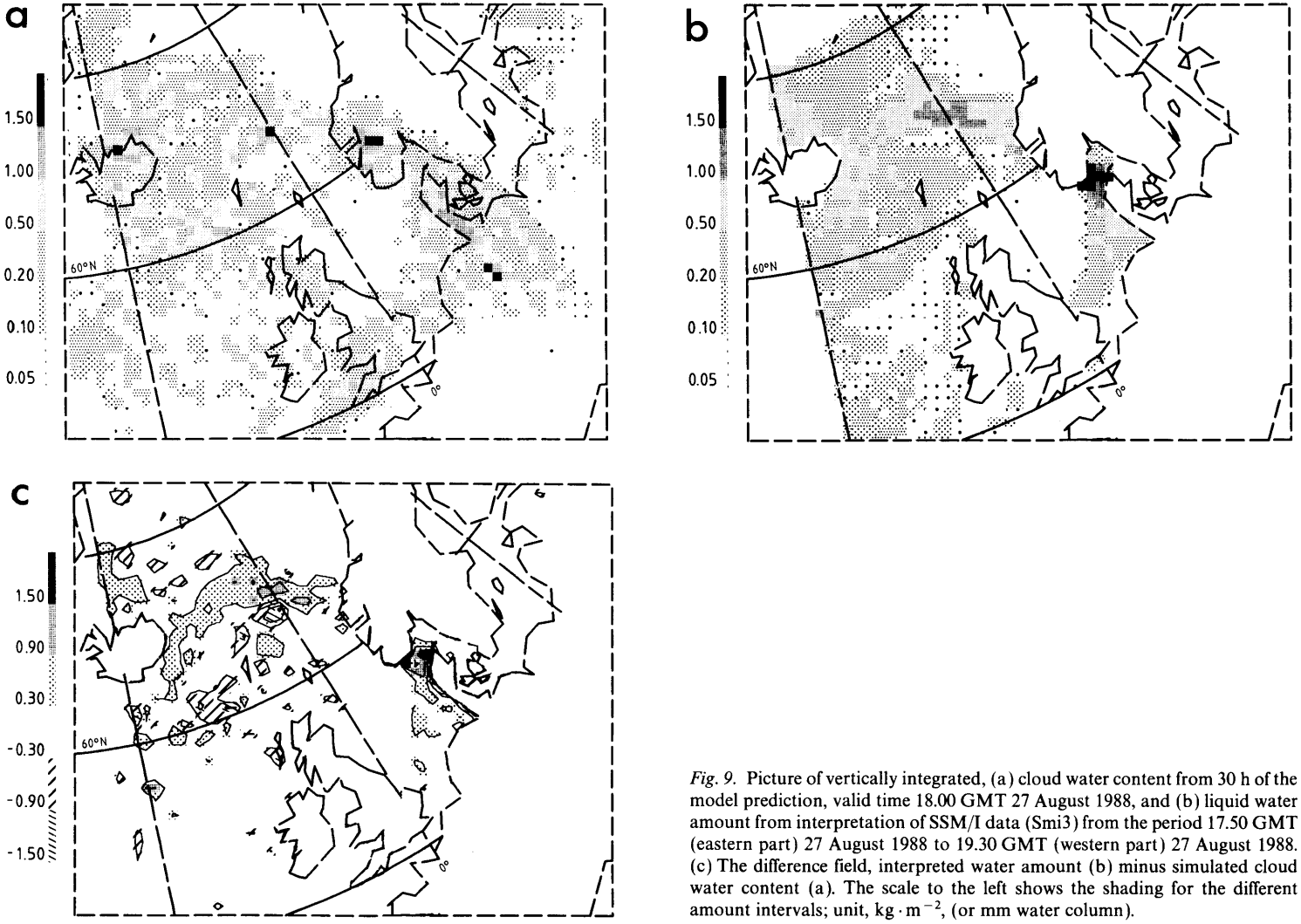

Fig. 9. Picture of vertically integrated, (a) cloud water content from 30 h of the model prediction, valid time 18.00 GMT 27 August 1988, and (b) liquid water amount from interpretation of SSM/I data (Smi3) from the period 17.50 GMT (eastern part) 27 August 1988 to 19.30 GMT (western part) 27 August 1988. (c) The difference field, interpreted water amount (b) minus simulated cloud water content (a). The scale to the left shows the shading for the different amount intervals; unit, $kg \cdot m^{-2}$, (or mm water column).

considerably brighter on the same side of the picture as where the sun is, as seen from the satellite. This has to do with the anisotropy in the bidirectional reflectivity, as reported by Taylor and Stowe (1984). When calculating the LWC from the satellite data, we have regarded the clouds as isotropic reflectors, so the anisotropy may explain some features that seem somewhat unrealistic. For example, from Fig. 6c we see that, in the eastern part, the satellite derived LWC at 8.45 GMT is higher than the simulated one at +21 h. Correspondingly we see from Fig. 7 that the analysed LWC at 14.30 GMT is considerably higher than the simulated one at +27 h in the western part. Those substantial positive deviations may in part be explained by the anisotropy, but it is apparent that some of them are due to underestimates in the model. For instance, the synoptic map at 09.00 GMT shows a rainband over West Germany and the synoptic map at 15.00 GMT shows a rain area over southern England and to the south of Iceland. The relatively high values of LWC from the satellite analysis are thus indirectly corroborated by other observations, while the simulated precipitation is nearly negligible in the same areas. The area of positive difference in Fig. 7, extending from about 0E, 62N southward along the west coast of Norway, may be explained by the fact that the precipitating water is not included in the model LWC. The simulated 3 h precipitation at +27 h is significant in this area. Most of the alternating positive and negative differences in the North Sea in Fig. 6c are due to the later time of the analysed frontal cloud band compared to the simulated cloud band in this area.

3.4. Cloud water content from model and SSM/I measurements

The LWC derived from the microwave data is compared with the vertical integral of predicted cloud water content. As indicated in Subsection 3.1, we have performed comparisons at three different points in time. As the results of those comparisons are essentially the same, we have chosen to show the results from the +30 h simulation (Fig. 9a) and Smi3 (Fig. 9b). The difference, Smi3 minus the simulation, is exhibited in Fig. 9c. The comparison is relevant only over the sea, since the microwave interpretation only exists there. It is seen that even in the +30 h forecast, there is remarkably good agreement between the positions of the frontal bands in Figs. 9a and 9b. An area of positive differences over Skagerack west of Sweden is seen in Fig. 9c. According to the synoptic map of 18.00 GMT, it is raining over that area, thus indicating that the numerical forecast underestimates the LWC. East of Iceland there is a band of positive differences, and a somewhat less coherent negative one south of that band. This situation indicates that the simulated system has a phase lag. However, this may, to some extent, be fictitious since the western part of the satellite analysis is from the satellite pass at about 19.30 GMT.

4. Summary

In the present study, cloud cover and cloud water content from a NWP model have been compared to the corresponding quantities derived from radiances measured by AVHRR and SSM/I on satellites. It is demonstrated that this type of retrieved meteorological parameters constitute potentially useful data samples for quantitative verification of model simulations. The results obtained in this pilot exercise are indeed encouraging. But there are some weaknesses in the retrieval methods that have to be removed before we can have sufficient confidence in the data to make quantitative verification meaningful. For instance in the retrieval methods applied to AVHRR data, it is necessary to treat the anisotropic reflectance more accurately. The constraint that the sun elevation is above a certain limit should be eliminated. The results of the present study indicate that the interpreted cloud cover in convective areas may have an unsatisfactory uncertainty. Furthermore, the inability to distinguish between snow cover and clouds is a very important difficulty that has to be removed so that the method can be applied with confidence at all times of the year.

As for the liquid water content, there is no straightforward answer to what is the best estimate, the simulation or the analysis. However, by utilizing precipitation reports on synoptic maps, we have some possibility to make a judgement over areas where the simulation and analysis have clear differences.

It is necessary that data from direct measurements (e.g., from FIRE and alike) are

utilized for calibration of the retrieved cloud parameters. To allow calibration of interpretations of microwave data, it is desirable that some dedicated field experiment is undertaken over ocean areas. Cloudiness produced in model simulations may also be compared with data from in situ measurements; an estimate of the simulated water content in the cloud proper is obtained by dividing the integrated water amount of a grid column with the associated cloud cover.

Despite uncertainties in the observational data considered here, it has yet been possible to infer some weaknesses in the model's parameterization scheme, by regarding the quantitative differences between analysis and simulation. Hence, it is found that the scheme has difficulties in handling the extremes of cloud cover in stratiform situations; there appears to be an underestimate of the cases with 100% cover and an overestimate of cloud-free areas.

Extensive utilization of the potential that retrieved cloudiness from satellite measurements represent will lead to improvements and refinements in the interpretation methods. So the sooner we begin to make use of those data, the sooner we will acquire a satisfactory level of accuracy and confidence in the retrieved data. In turn, this will facilitate improvements and refinements in the condensation-cloud parameterization schemes. As our parameterization schemes improve, we can utilize them to derive the vertical distribution of condensation and cloud processes. It will then be possible to improve the humidity analysis as well as to establish initial states of release of latent heat and of cloud water content. A confident description of the latent heating is of great value in the initialization process. As more advanced condensation-cloud schemes become adopted in prediction models, it will be of great importance (e.g., for minimizing spin-up) that a realistic initial state of cloud water content is given.

5. Acknowledgments

We thank Nils Gunnar Kvamstø for programming assistance and for performing the model simulations. We appreciate the assistance of G. W. Petty and D. K. Miller in producing the microwave integrated liquid water data. We also wish to thank Mr. Øyvind Thomassen for programming assistance and Mr. Frank Cleveland for preparing the figures. The SSM/I brightness temperatures were kindly provided by F. Wentz and E. Francis of Remote Sensing Systems, Inc. We gratefully acknowledge the computer resources that were provided free of charge by Bergen Scientific Centre (BSC/IBM). The work by E. R. and H. S. has been supported by The Norwegian Research Council for Science and Humanities under Contract ABC/SDU 447.89/008. The work at University of Washington was supported by NASA Grants NAGW-1688 and NAG5-943.

6. Appendix

List of ACRONYMS

AMUB	Section of Meteorology, University of Bergen
AVHRR	Advanced Very High Resolution Radiometer
BSC	Bergen Scientific Centre (IBM)
CFL	Courant-Friedrichs-Levy (numerical stability condition)
CWC	Cloud Water Content
FIRE	First ISCCP Regional Experiment
GCM	General Circulation Model
ISCCP	International Satellite Cloud Climatology Project
LWC	Liquid Water Content
NRSC	Nansen Remote Sensing Center
NWP	Numerical Weather Prediction
SMMR	Scanning Multichannel Microwave Radiometer
SSM/I	Special Sensor Microwave Imager

REFERENCES

Arking, A. and Childs, J. D. 1985. Retrieval of Cloud Cover Parameters from Multispectral Satellite Images. *J. Clim. and Appl. Meteor. 24*, 322–333.

Bratseth, A. M. 1983. Some economical, explicit finite-difference schemes for the primitive equations. *Mon. Wea. Rev. 111*, 663–668.

Cess, R. D., Potter, G. L., Blanchet, J. P., Boer, G. J., Gahn, S. J., Kiehl, J. T., Le Treut, H., Liang, Z.-X.,

Mitchell, J. F. B., Morcrette, J.-J., Randall, D. A., Riches, M. R., Röckner, E., Schlese, U., Slingo, A., Taylor, K. E., Washington, W. M., Weatherald, R. T. and Yagai, I. 1989. Interpretation of cloud-climate feedback as produced by 14 atmospheric general circulation models. *Science 245*, 513–516.

Coakley, J. A. and Chylek, P. 1975. The two-stream approximation in radiative transfer: including the angle of the incident radiation. *J. Atmos. Sci. 32*, 409–418.

Cox, S. K., McDougal, D., Randall, D. A. and Schiffer, R. A. 1987. FIRE-The First ISCCP regional experiment. *Atmosphere, Ocean 67*, 114–118.

Curry, J. A., Ardeel, C. D. and Tian, L. 1990. Liquid Water Content and Precipitation Characteristics of Stratiform Clouds as Inferred from Satellite Microwave Measurements. *J. Geophys. Res. 95*, 16659–16671.

Grønås, S., Foss, A. and Lystad, M. 1987. Numerical simulations of polar lows in the Norwegian Sea. *Tellus 39A*, 334–353.

Katsaros, K. B., Bhatti, I., McMurdie, L. A. and Petty, G. W. 1989. Identification of atmospheric fronts over the ocean with microwave measurements of water vapor and rain. *Weather and Forecasting 4*, 449–460.

Katsaros, K. B., Hammarstrand, U. and Petty, G. W. 1990. Atmospheric water in mid-latitude cyclones observed by microwave radiometry and compared to model calculations. *Report DM-52*. Department of Meteorology, Stockholm University, S-106 91 Stockholm, Sweden.

Manabe, S. and Stouffer, R. J. 1980. Sensitivity of a global climate model to an increase of CO_2-concentration in the atmosphere. *J. Geophys. Res. 85*, 5529–5554.

McMurdie, L. A. and Katsaros, K. B. 1985. Atmospheric water distribution in a mid-latitude cyclone observed by the Seasat Scanning Multichannel Microwave Radiometer. *Mon. Wea. Rev. 113*, 584–598.

Nordeng, T. E. 1986. Parameterization of physical processes in a three-dimensional numerical weather prediction model. *Tech. Rep. no. 65*. The Norwegian Meteorological Institute, Oslo, Norway.

Petty, G. W. 1990. *On the response of the Special Sensor Microwave/Imager to the marine environment—Implications for atmospheric parameter retrievals.* Ph.D. Thesis. Dept. of Atmospheric Sci., University of Washington. (Available from University Microfilms, 300 North Zeeb Road, Ann Arbor, Michigan 48106, USA, pp. 291.)

Ramanathan, V. E., Pitcher, E. J., Malone, R. C. and Blackmon, M. L. 1983. The response of a spectral general circulation model to refinements in radiative processes. *J. Atmos. Sci. 40*, 605–630.

Raustein, E. 1989. Use of a clustering method for objective cloud classification and determination of cloud parameters from satellite data. *Report NR: 2, 1989.* Meteorological Report Series, University of Bergen. (Available from Geophysical Institute, University of Bergen, Allégt. 70, N-5007 Bergen, Norway.)

Röckner, E. and Schlese, U. 1987. Cloud optical depth feedbacks and climate modelling. *Nature 329*, 10 September, 138–140.

Saunders, R. W. 1989. A comparison of Satellite-retrieved Parameters with Mesoscale Model Analyses. *Quart. J. Roy. Meteor. Soc. 115*, 651–672.

Slingo, A. and Slingo, J. M. 1988. The response of a general circulation model to cloud longwave radiation forcing. I: Introduction and initial experiments. *Quart. J. Roy. Meteor. Soc. 114*, 1027–1062.

Slingo, A. 1990. Sensitivity in the earth's radiation budget to changes in low clouds. *Nature 343*, 4 January 1990, 49–51.

Staelin, D. H., Kunzi, K. F., Pettyjohn, R. L., Poon, R. K. L. and Wilcox, R. W. 1976. Remote sensing of atmospheric water vapor and liquid water with the Nimbus 5 microwave spectrometer. *J. Appl. Meteor. 15*, 1204–1214.

Stephens, G. L. 1978. Radiation Profiles in extended Water Clouds. II: Parameterization Schemes. *J. Atmos. Sci. 35*, 2123–2132.

Sundqvist, H. 1988. Parameterization of condensation and associated clouds in models for weather prediction and general circulation simulation. In: *Physically-based modelling and simulation of climate and climatic change*, (ed. M. E. Schlesinger), Reidel, Dordrecht. Part 1, 433–461.

Sundqvist, H., Berge, E. and Kristjánssón, J. E. 1989. Condensation and cloud parameterization studies with a mesoscale numerical weather prediction model. *Mon. Wea. Rev. 117*, 1641–1657.

Takeda, T. and Liu, G. 1987. Estimation of atmospheric liquid-water amount by NIMBUS 7 SMMR data: A new method and its application to the western North-Pacific region. *J. Meteor. Soc. Japan 65*, 931–947.

Taylor, V. R. and Stowe, L. L. 1984. Atlas of reflectance patterns for uniform earth and cloud surfaces. *NOAA Technical Reports, NESDIS 10.*

Tian, L. and Curry, J. A. 1989. Cloud overlap statistics. *J. Geophys. Res. 94*, D7, 9925–9935.

Wetherald, R. J. and Manabe, S. 1988. Cloud feedback processes in a general circulation model. *J. Atmos. Sci. 45*, 1397–1415.